Far field intensity distributions due to spatial self phase modulation of a Gaussian beam by a thin nonlocal nonlinear media

E. V. Garcia Ramirez,[1,*] M. L. Arroyo Carrasco,[1] M. M. Mendez Otero,[1] S. Chavez Cerda,[2] M. D. Iturbe Castillo[2]

[1]*Facultad de Ciencias Físico-Matemáticas, Benemérita Universidad Autónoma de Puebla, Av. San Claudio y 18 Sur. Col San Manuel,C.P. 72570, Puebla, Puebla, México.*

[2]*Instituto Nacional de Astrofísica, Óptica y Electrónica, Luis Enrique Erro # 1, C.P. 72840 Tonantzintla, Puebla, México.*

[*]*emma_vgr@yahoo.com.mx*

Abstract: In this work we present a simple model that can be used to calculate the far field intensity distributions when a Gaussian beam cross a thin sample of nonlinear media but the response can be nonlocal.

OCIS codes: (190.0190) Nonlinear optics; (190.5940) Self-action effects; (190.4420) Transverse effects in nonlinear optics.

References and links

1. W. R. Callen, B. G. Huth, and R. H. Pantell, "Optical patterns of thermally self-defocused light," Appl. Phys. Lett. **11**(3), 103–105 (1967).
2. F. W. Dabby, T. K. Gustafson, J. R. Whinnery, and Y. Kohanzadeh, "Thermally self-induced phase modulation of laser beam," Appl. Phys. Lett. **16**(9), 362–365 (1970).
3. S. D. Durbin, S. M. Arakelian, and Y. R. Shen, "Laser-induced diffraction rings from a nematic-liquid-crystal film," Opt. Lett. **6**(9), 411–413 (1981).
4. E. Santamato, and Y. R. Shen, "Field-curvature effect on the diffraction ring pattern of a laser beam dressed by spatial self-phase modulation in a nematic film," Opt. Lett. **9**(12), 564–566 (1984).
5. R. G. Harrison, L. Dambly, D. Yu, and W. Lu, "A new self-diffraction pattern formation in defocusing liquid media," Opt. Commun. **139**(1-3), 69–72 (1997).
6. A. Shevchenko, S. C. Buchter, N. V. Tabiryan, and M. Kaivola, "Creation of a hollow laser beam using self-phase modulation in a nematic liquid crystal," Opt. Commun. **232**(1-6), 77–82 (2004).
7. D. Yu, W. Lu, R. G. Harrison, and N. N. Rosanov, "Analysis of dark spot formation in absorbing liquid media," J. Mod. Opt. **45**, 2597–2606 (1998).
8. S. Brugioni, and R. Meucci, "Self-phase modulation in a nematic liquid crystal film induced by a low-power CO_2 laser," Opt. Commun. **206**(4-6), 445–451 (2002).
9. L. Lucchetti, S. Suchand, and F. Simoni, "Fine structure in spatial self-phase modulation patterns: at a glance determination of the sign of optical nonlinearity in highly nonlinear films," J. Opt. A, Pure Appl. Opt. **11**(3), 034002 (2009).
10. L. Deng, K. He, T. Zhou, and C. Li, "Formation and evolution of far-field diffraction patterns of divergent and convergent Gaussian beams passing through self-focusing and self-defocusing media," J. Opt. A, Pure Appl. Opt. **7**(8), 409–415 (2005).
11. C. M. Nascimento, M. Alencar, S. Chávez-Cerda, M. Da Silva, M. R. Meneghetti, and J. M. Hickmann, "Experimental demonstration of novel effects on the far-field diffraction patterns of a Gaussian beam in a Kerr medium," J. Opt. A, Pure Appl. Opt. **8**(11), 947–951 (2006).
12. F. W. Dabby, and J. R. Whinnery, "Thermal self-focusing of laser beams in lead glasses," Appl. Phys. Lett. **13**(8), 284–286 (1968).
13. M. Segev, B. Crosignani, A. Yariv, and B. Fischer, "Spatial solitons in photorefractive media," Phys. Rev. Lett. **68**(7), 923–926 (1992).
14. D. Suter, and T. Blasberg, "Stabilization of transverse solitary waves by a nonlocal response of the nonlinear medium," Phys. Rev. A **48**(6), 4583–4587 (1993).
15. W. Królikowski, and O. Bang, "Solitons in nonlocal nonlinear media: Exact solutions," Phys. Rev. E Stat. Phys. Plasmas Fluids Relat. Interdiscip. Topics **63**(1), 016610 (2000).
16. Y. R. Shen, The principles of nonlinear optics (Wiley classics library, 2003). Chap. 17.
17. M. Born, and E. Wolf, Principles of Optics (Oxford:Pergamon, 1980). Chap. 8.
18. W. Krolikowski, O. Bang, N. I. Nikolov, D. Neshev, J. Wyller, J. J. Rasmussen, and D. Edmundson, ""Modulational instability, solitons and beam propagation in spatially nonlocal nonlinear media," J. Opt. B Quantum Semiclass. Opt. **6**, S288–S294 (2004).
19. E. W. Van Stryland, and D. Hagan, "Measuring nonlinear refraction and its dispersion" in Self-focusing: past and present, R.W. Boyd, S.G. Lukishova Bad, Y.R. Shen, Eds. (Springer, 2009) 573–591.

#130856 - $15.00 USD Received 7 Jul 2010; revised 13 Aug 2010; accepted 15 Sep 2010; published 4 Oct 2010

20. S. A. Akhmanov, D. P. Krindach, A. P. Sukhorukov, and R. V. Khokhlov, "Nonlinear defocusing of laser beams," JEPT Lett. **6**, 38 (1967).

1. Introduction

When a material presents an intensity dependent refractive index then it can change dramatically an incident beam with a well defined distribution. Typically a ring pattern can be observed at far field when a Gaussian distribution illuminates a thin sample of the nonlinear material. This phenomena known as spatial self phase modulation, has been studied for many research groups, whom had given different theoretical models to describe the observed patterns. The first observation of this effect was reported by Callen *et al* [1] in 1967, when they illuminated a CS_2 sample with a He-Ne beam. In 1970 Dabby *et al* [2] presented a qualitative and quantitative study of the phenomena. A similar effect was observed in liquid crystals by Durbin *et al* [3] in 1981. Santamato and Shen [4] proposed that the far field pattern was composed by two sets of concentric rings: one due to the nonlinearity and the other one to the interference between self-phase modulation and wavefront curvature. This nonlinear effect has been observed in numerous materials [1–9]. The main difference is on the central portion of the far field pattern, in some cases is dark [5–7], while in others is brilliant [8,9]. Many papers involve experimental and numerical results [9–11]. Recently a method based on the far field intensity distributions has been proposed to determine the sign of the nonlinear refractive index of highly nonlinear samples [9], where the z-scan technique is not adequate.

Assuming steady state conditions, the nonlocality is a mechanism that spread out or in localized excitations. The physical mechanism that creates such response can be of different origins: heat [12], charge carriers [13], atoms [14], etc. Nonlocality has been considered in the propagation of optical beams in some materials [15], however has not been considered in general to explain spatial self phase modulation of Gaussian beams by thin samples.

In this work we propose a simple model where the locality in the nonlinear response of the material is taking into account. We demonstrate that the features of the far field pattern are affected by the nonlocality, magnitude of the maximum on axis nonlinear phase shift and position of the sample.

In the next section we present our theoretical model and the main suppositions that must be fulfilled in order to calculate the far field patterns. Then some numerical results are presented taking into account the main parameters that affect such distribution. Finally the conclusions are presented.

2. Theoretical model

We are going to consider a Gaussian beam of waist w_0 and wavelength λ, propagating in the z direction. This beam has a Rayleigh range z_0 given by $z_0 = \pi w_0^2 / \lambda$, and the following field amplitude:

$$E(r,z) = A_0 \frac{w_0}{w(z)} \exp\left[-\frac{r^2}{w(z)^2} \right] \exp\left[-ikz - ik\frac{r^2}{2R(z)} + i\varepsilon(z) \right], \tag{1}$$

Where;

$$w(z) = w_0 \left[1 + \left(z / z_0 \right)^2 \right]^{1/2}, \tag{2}$$

$$R(z) = z \left[1 + \left(z_0 / z \right)^2 \right], \tag{3}$$

$$\varepsilon(z) = \tan^{-1}\left(z / z_0 \right), \tag{4}$$

#130856 - $15.00 USD Received 7 Jul 2010; revised 13 Aug 2010; accepted 15 Sep 2010; published 4 Oct 2010

where A_0 is a constant, $k = 2\pi/\lambda$, $w(z)$ and $R(z)$ are the beam width and wavefront radius of curvature, respectively and $\varepsilon(z)$ is the phase retardation relative to a plane wave.

At some distance z from the waist the beam illuminates an optical nonlinear sample of width d. This sample is going to be considered as thin ($d<<z_0$) and that present a refractive index dependent on the incident intensity. It is well accepted that when a Gaussian beam illuminates such samples then the output field can be expressed by [10]:

$$E_{out} = E(r,z)\exp\left(-i\Delta\varphi(r)\right), \tag{5}$$

where we are considering that the sample has not absorption. E is the field amplitude of the Gaussian beam at the entrance of the sample, r the radial coordinate and $\Delta\varphi(r)$ the nonlinear phase change. This nonlinear phase change can be approximated as [3,10];

$$\Delta\varphi(r) \approx \Delta\varphi_0 \exp\left(-2r^2/w^2\right), \tag{6}$$

here, $\Delta\varphi_0$ is the maximum on axis phase shift photo-induced in the beam after crossing the nonlinear medium set at z. This phase change is due to the intensity-dependent refractive index of the material. If $\Delta\varphi_0$ is much larger than 2π [16], a pattern of concentric rings appear at far field, Fresnel-Kirchhoff diffraction formula can be used to evaluate the intensity distribution at far field [17].

In order to describe the response of the material in some cases it is necessary to solve one differential equation for the field and another one for the material. Nevertheless, Eq. (6) describes very well the far field patterns observed for materials with a spatial local response. However, not all the materials present such response. In this work we propose a very simple model to describe the far field intensity distribution that can be obtained when the response of the material is nonlocal. We propose that the nonlocality can be considered as a number m in the following expression for the nonlinear phase shift:

$$\Delta\varphi(r) \approx \Delta\varphi_0 \exp\left(-mr^2/w^2\right) = \Delta\varphi_0 \exp\left(-r^2/\left(w/\sqrt{m}\right)^2\right), \tag{7}$$

where m can be any real positive number. Note that m can be considered as a factor that affects the width of the Gaussian function (last expression in Eq. (7)). For $m<2$ the nonlinear phase change extend beyond the incident intensity distribution and for $m>2$ the nonlinear phase change is narrower than the intensity distribution. Only for $m = 2$ the nonlinear phase change follows the intensity distribution and then the response of the material is considered as local. Values of m different of 2, in Eq. (7), will be considered as nonlocal.

The previous equation can be obtained considering that the phase shift is directly proportional to the change of the refractive index $N(I)$, that in the case of a nonlocal media the following phenomenological expression is used [18];

$$N(I) = s\int R(\xi - r)I(\xi,z)d\xi, \tag{8}$$

where s is positive (negative) for a self-focusing (self-defocusing) nonlinear media, I is the intensity of the incident beam $(I(r,z) = |E(r,z)|^2)$ and R, a real localized and symmetric function, is the response function of the nonlocal medium whose width determines the degree of nonlocality [15]. This phenomenological function (Eq. (8)) describes several real physical situations according to references [15,18].

The Eq. (8) is the correlation between functions R and I, in our case we are considering that I is Gaussian. For the function R we will consider two cases: 1) a delta function and 2)

#130856 - $15.00 USD Received 7 Jul 2010; revised 13 Aug 2010; accepted 15 Sep 2010; published 4 Oct 2010

another Gaussian function [3]. In the first case, $R(r) = \delta(r)$ the response is local, the resulting change of the refractive index is directly proportional to I and, in our model, this corresponds to $m = 2$ in Eq. (7). In the second case the correlation gives a Gaussian function. For the Gaussian response with a given width, if this is smaller than the extension of the beam it is said that there exists a weak nonlocality (in our model $m>2$). When the width of the response function is much wider than the incident beam the case is called highly nonlocal [15,18]. In our model $m<2$ mean that the refractive index change extends beyond the incident intensity. Finally, a Gaussian response is valid as shown by Shen and associates [3], who used a similar expression to Eq. (7) for the induced phase shift observed in their experiments. Thus, from the correlation in Eq. (8) with a Gaussian response we conclude that nonlocality can be modeled by considering a Gaussian phase shift with different values of m in Eq. (7).

In the next section we show numerical results obtaining the Fourier transform of the field given by Eq. (5), considering Eq. (7), for different values of m and different positions z of the sample, which are normalized to the Rayleigh range z_0 and analyze the far field patterns for different maximum phase shifts. The results will be presented in graphs with the same coordinates as the figures in reference [10].

3. Numerical results

We are going to present a study where the position of the thin nonlinear sample was changed and two different magnitudes of the on axis nonlinear phase change were considered. From a z-scan experiment, where the far field on axis transmittance is measured as a function of the position, for a thin Kerr material we know that the nonlinear response can be exhibited at distances far from the waist as large as $6z_0$ [19]. The maximum changes in the transmitted intensity of the sample in a z-scan experiment are obtained for distances close to z_0 from the waist. For these reasons the positions for the sample considered in this characterization are $z = 4z_0$, $2z_0$, z_0 and $z = 0$. Furthermore, for those positions is very simple to calculate $w(z)$ and $R(z)$ from Eqs. (2) and (3), respectively. Two values of the maximum nonlinear phase shift are considered, one in the lower limit (2π rad) where the formation of one ring is expected at the far field and the other one (12π rad) where many rings must be clearly distinguished.

For a positive nonlinear phase change $\Delta\varphi_0 = 2\pi$ rad and the sample set before the waist of the incident Gaussian beam, $z = -4z_0$ (convergent beam), the patterns present the following characteristics: the diameter of the spot is almost the same for all cases, the beam present a minimum in the center; this minimum is smaller as m increases, such that a well defined ring is obtained at far field for $m = 4$ and not for $m = 1$, see Fig. 1.

#130856 - $15.00 USD Received 7 Jul 2010; revised 13 Aug 2010; accepted 15 Sep 2010; published 4 Oct 2010

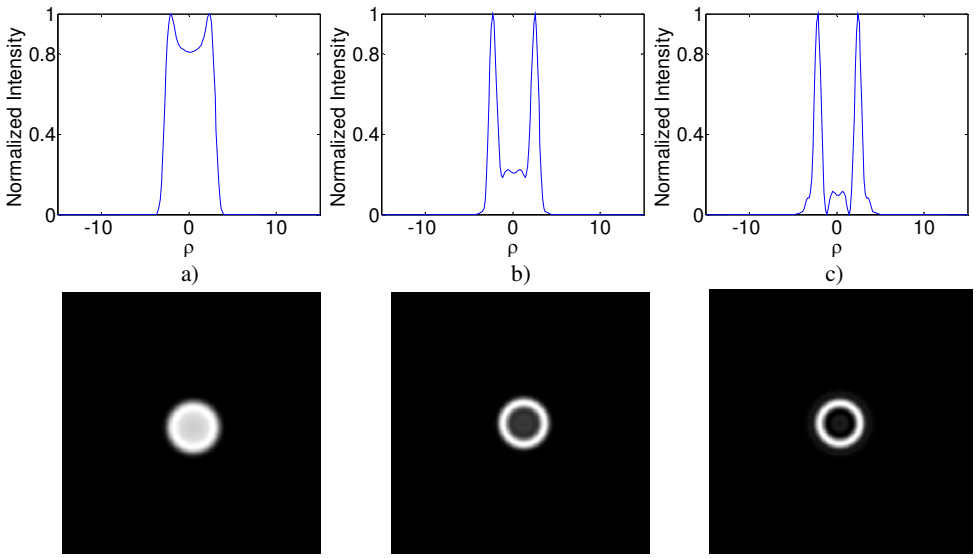

Fig. 1. Far field intensity profiles (upper row) and cross sections (lower row) obtained for a sample with $\Delta\varphi_0 = 2\pi$ rad, set at $z = -4z_0$. And different values of m: a) 1, b) 2 and c) 4.

At the same position and for $\Delta\varphi_0 = 12\pi$ rad the far field patterns present the following characteristics: The diameter and number of rings increased with the value of m; a central dark spot is obtained in all cases but its diameter is smaller as m increases. The outermost ring was of the highest intensity for $m = 1$ and 2, but not for $m = 4$, where the highest intensity ring surround the central dark spot, see Fig. 2.

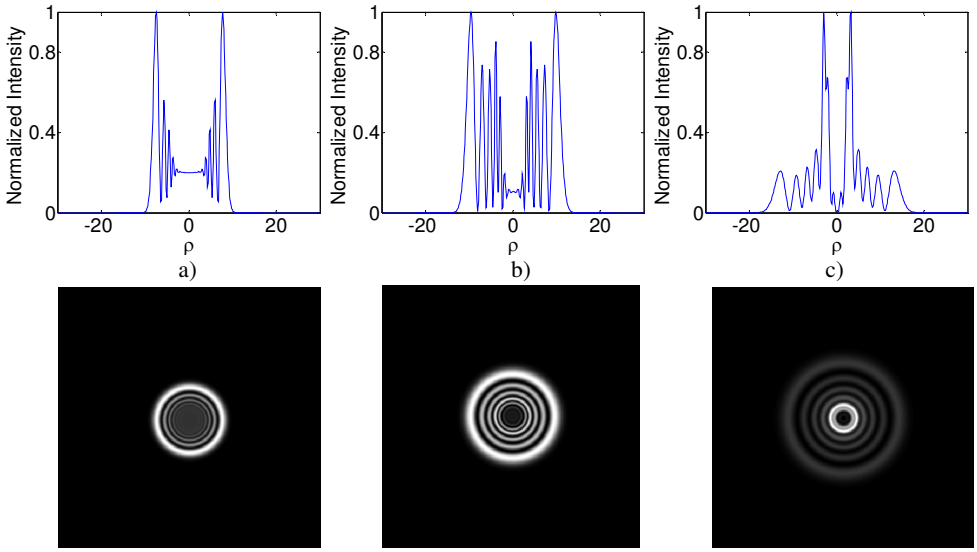

Fig. 2. Far field intensity profiles (upper row) and cross sections (lower row) obtained for a sample with $\Delta\varphi_0 = 12\pi$ rad, set at $z = -4z_0$. And different values of m: a) 1, b) 2 and c) 4.

Changing the position of the sample, keeping the same sign for the wavefront curvature radius remarkable differences can appear in the far field patterns. For example at $z = -2z_0$ and $\Delta\varphi_0 = 2\pi$ rad the following differences are noted: a central bright spot appears for $m = 2$ and

#130856 - $15.00 USD Received 7 Jul 2010; revised 13 Aug 2010; accepted 15 Sep 2010; published 4 Oct 2010

4, see Fig. 3. This result is very important due to contradict the main conclusion of references [9,10] in order to identify the sign of the nonlinearity. Another difference was in the spatial extension of the pattern that was larger than in the previous position.

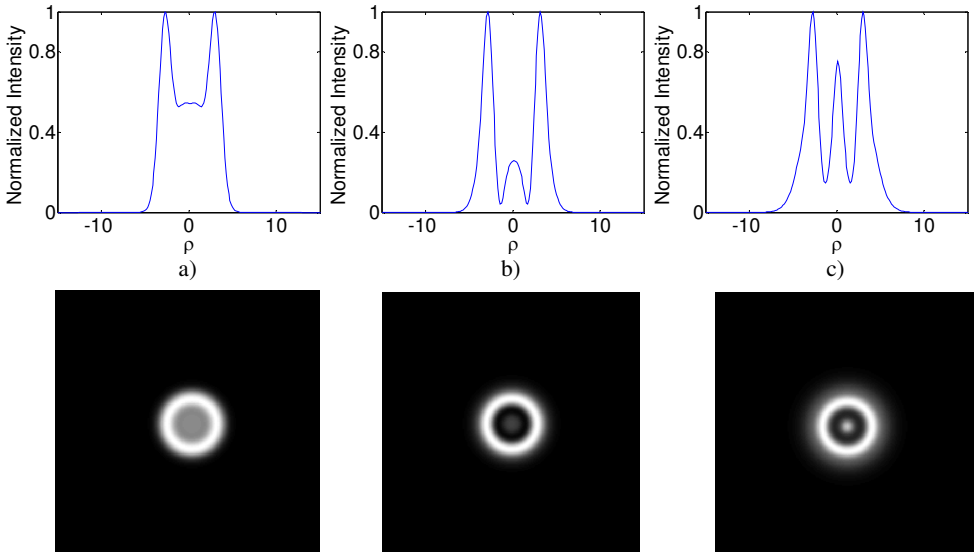

Fig. 3. Far field intensity profiles (upper row) and cross sections (lower row) obtained for a sample with $\Delta\varphi_0 = 2\pi$ rad, set at $z = -2z_0$. And different values of m: a) 1, b) 2 and c) 4.

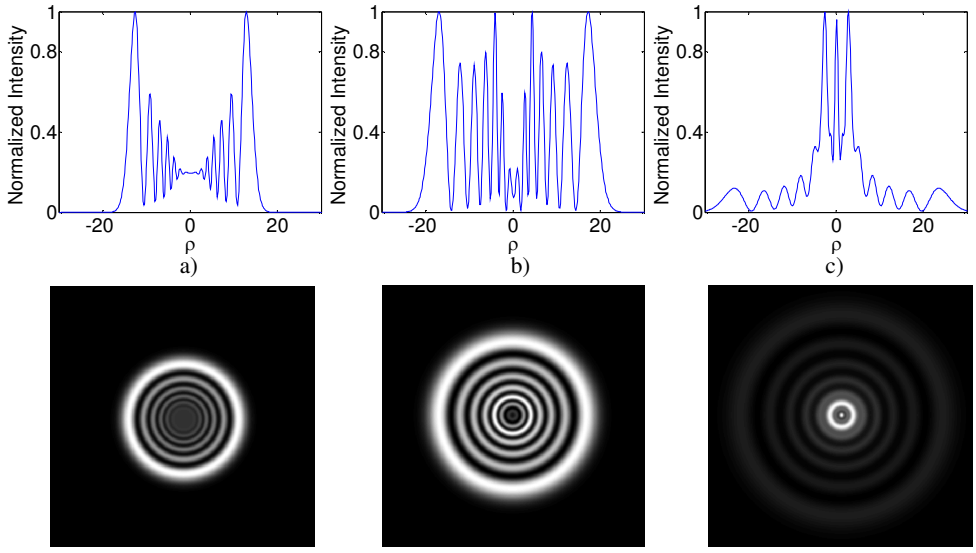

Fig. 4. Far field intensity profiles (upper row) and cross sections (lower row) obtained for a sample with $\Delta\varphi_0 = 12\pi$ rad, set at $z = -2z_0$. And different values of m: a) 1, b) 2 and c) 4.

#130856 - $15.00 USD Received 7 Jul 2010; revised 13 Aug 2010; accepted 15 Sep 2010; published 4 Oct 2010

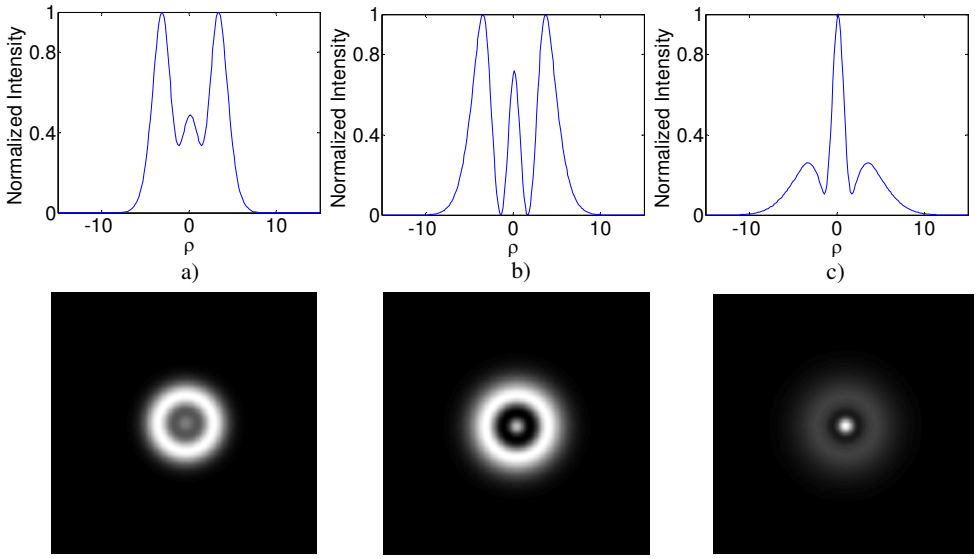

Fig. 5. Far field intensity profiles (upper row) and cross sections (lower row) obtained for a sample with $\Delta\varphi_0 = 2\pi$ rad, set at $z = -z_0$. And different values of m: a) 1, b) 2 and c) 4.

For the sample with $\Delta\varphi_0 = 12\pi$ rad the far field patterns presented the following characteristics, see Fig. 4: many rings were observed but only for the case $m = 2$ they present good contrast. The spatial extension of the pattern was larger than in the previous position. For $m = 1$ outermost ring had the maximum intensity and contrast, the inner rings had low contrast. For $m = 4$ the number of observed rings was smaller than for $m = 2$, and the ring closer to the center was the most intense. It seems that the pattern present two set of rings, one with higher frequency and intensity than the other. A central bright spot was obtained for this value of m. Here is important to mention that even though the phase shift is the same for all cases the number of rings were not the same for the different patterns with different values of m.

In Fig. 5 we present the far field patterns obtained for a sample set at $z = -z_0$ with $\Delta\varphi_0 = 2\pi$ rad. In this case all the patterns presented a central bright spot and one ring surrounding it, the intensity of this central spot was larger with respect to the ring as m increases. Note that at this position $R(z)$ reaches its minimum value and its equal to $2z_0$.

In Fig. 6 we present the far field patterns obtained for a sample set at $z = -z_0$ with $\Delta\varphi_0 = 12\pi$ rad. Many rings with good contrast were obtained for $m = 1$ and 2, but for $m = 4$ low intensity rings were obtained. In all cases we can see a central bright spot. The spatial extension of the patterns was larger than in the previous positions. The number of observed rings was very close to that waited due to the magnitude of the on axis nonlinear phase change.

#130856 - $15.00 USD Received 7 Jul 2010; revised 13 Aug 2010; accepted 15 Sep 2010; published 4 Oct 2010

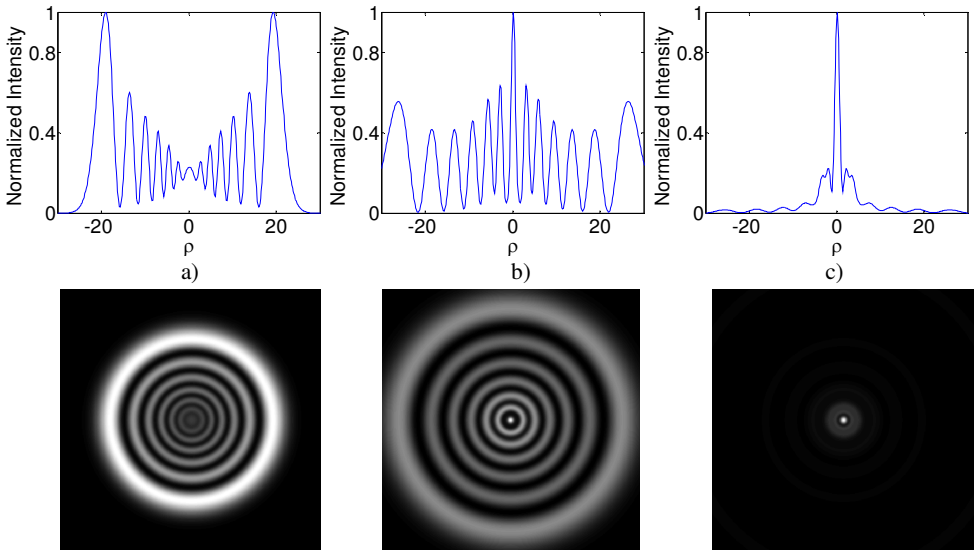

Fig. 6. Far field intensity profiles (upper row) and cross sections (lower row) obtained for a sample with $\Delta\varphi_0 = 12\pi$ rad, set at $z = -z_0$. And different values of m: a) 1, b) 2 and c) 4.

When the sample was set at the waist of the incident Gaussian beam, this means wavefronts without curvature; the patterns for the two magnitudes of the on axis nonlinear phase shift presented the characteristics shown in Figs. 7 and 8. Figure 7 shows the results obtained for a sample with $\Delta\varphi_0 = 2\pi$ rad, the characteristics of the patterns were the following: when $m = 1$, the pattern presents a central dark spot and for $m = 2$ and 4 there was a central bright spot surrounded by a ring. The intensity of the ring was smaller as m increase. The spatial extension of the pattern is slightly larger than in the previous position and grew as m does.

Figure 8 shows the results for the same position as in Fig. 7 with $\Delta\varphi_0 = 12\pi$ rad. Patterns with many rings were obtained for $m = 1$ and 2, however for $m = 4$ the pattern presented a central bright spot surrounded by one ring. The pattern obtained for $m = 1$ presents a central dark spot, it was well contrasted, the outermost ring had the higher intensity and the innermost the smaller intensity; the number of observed rings correspond to the phase shift. For $m = 2$ the pattern presented a central bright spot and the innermost ring presented the highest intensity, the rest of the rings had similar maximum intensity but very small compared with the central spot. The number of observed rings, for this value of m, corresponds to the phase shift.

#130856 - $15.00 USD Received 7 Jul 2010; revised 13 Aug 2010; accepted 15 Sep 2010; published 4 Oct 2010

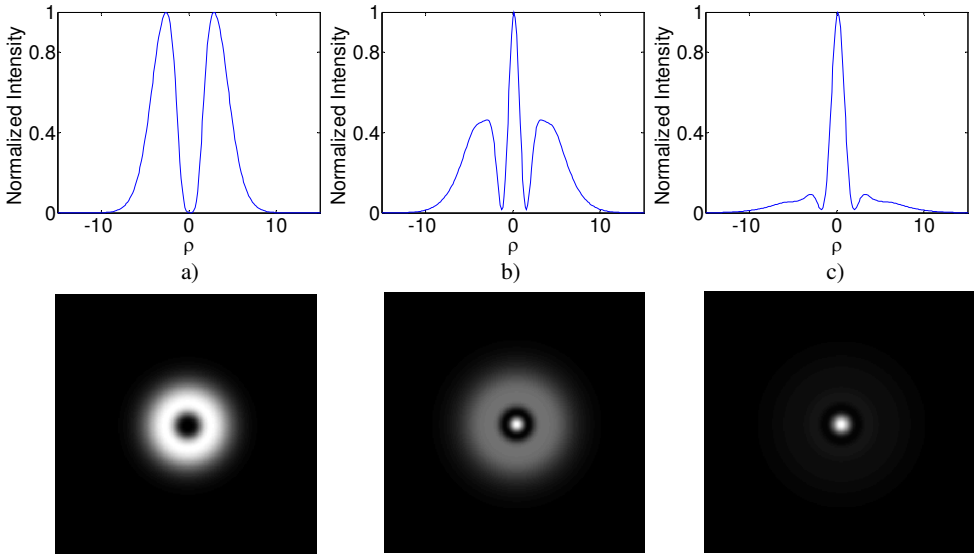

Fig. 7. Far field intensity profiles (upper row) and cross sections (lower row) obtained for a sample with $\Delta\varphi_0 = 2\pi$ rad, set at $z = 0$. And different values of m: a) 1, b) 2 and c) 4.

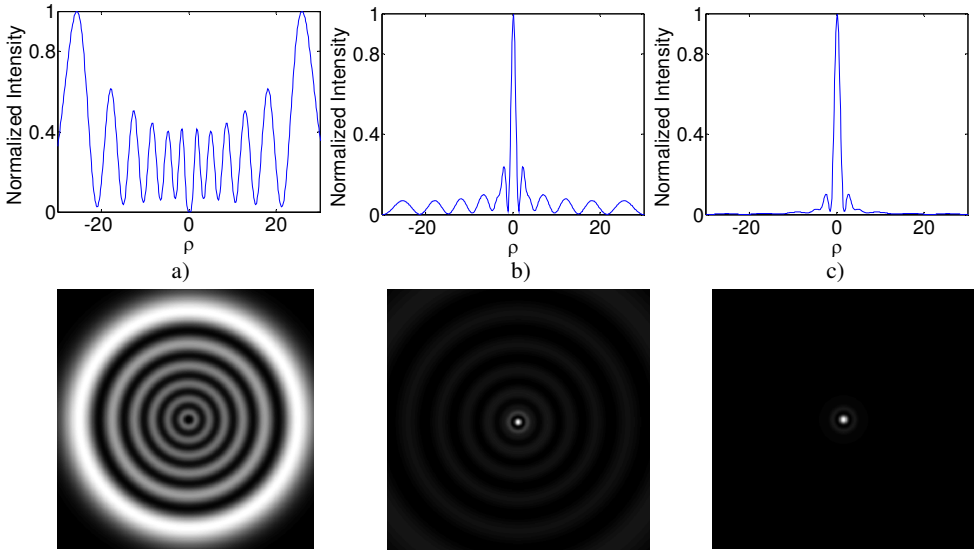

Fig. 8. Far field intensity profiles (upper row) and cross sections (lower row) obtained for a sample with $\Delta\varphi_0 = 12\pi$ rad, set at $z = 0$. And different values of m: a) 1, b) 2 and c) 4.

The rest of the positions presented in this work correspond to a divergent Gaussian beam. For the position $z = z_0$ with $\Delta\varphi_0 = 2\pi$ rad, the far field patterns presented the following characteristics: the diameter of the pattern grows with the increment of m, however was smaller than in the previous position. In all cases there was a central bright spot and one ring, see Fig. 9. The intensity of the central bright spot was larger than that of the ring.

#130856 - $15.00 USD Received 7 Jul 2010; revised 13 Aug 2010; accepted 15 Sep 2010; published 4 Oct 2010

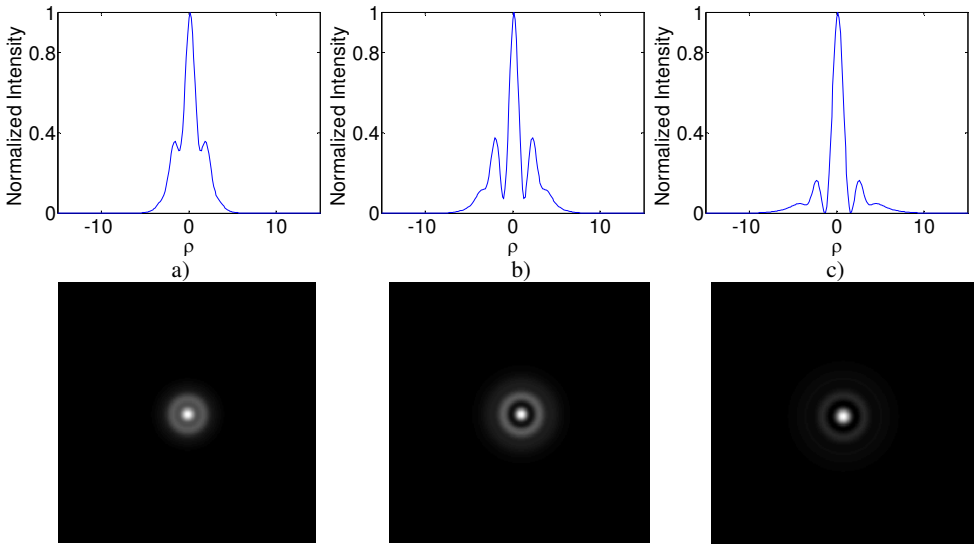

Fig. 9. Far field intensity profiles (upper row) and cross sections (lower row) obtained for a sample with $\Delta\varphi_0 = 2\pi$ rad, set at $z = z_0$. And different values of m: a) 1, b) 2 and c) 4.

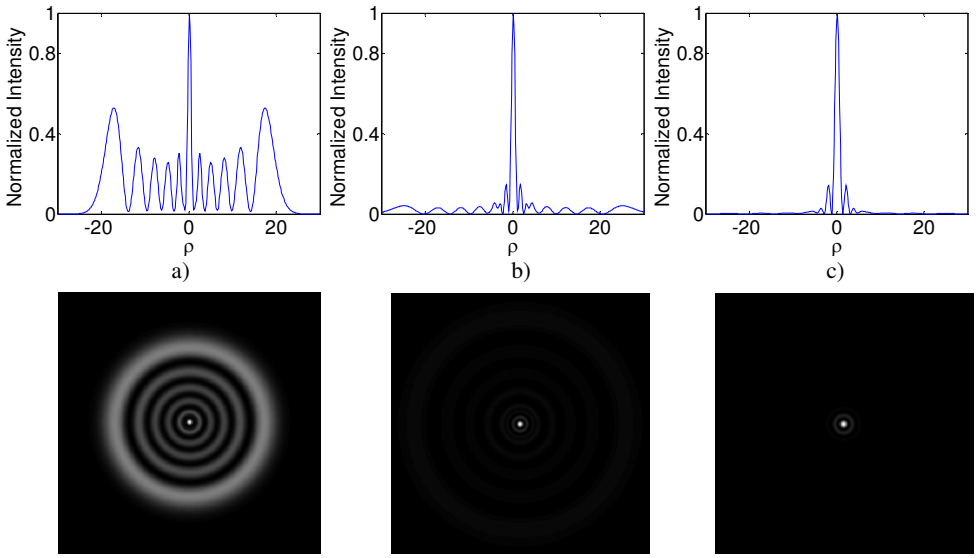

Fig. 10. Far field intensity profiles (upper row) and cross sections (lower row) obtained for a sample with $\Delta\varphi_0 = 12\pi$ rad, set at $z = z_0$. And different values of m: a) 1, b) 2 and c) 4.

In Fig. 10 we present the results obtained for a sample set at $z = z_0$ and $\Delta\varphi_0 = 12\pi$ rad. The far field patterns presented the following characteristics: a central bright spot for all cases, many rings were obtained for $m = 1$ and 2 but for $m = 4$ only one ring can be clearly observed. The rings observed for $m = 1$ presented good contrast and the outermost ring had the highest intensity. For $m = 2$ two set of rings were obtained one with high frequency and intensity and the other with low frequency and intensity.

When the sample was set at $z = 2z_0$ and $\Delta\varphi_0 = 2\pi$ rad, the far field pattern presented a central bright spot for all values of m. For $m = 2$ and 4 this central bright spot was surrounded

#130856 - $15.00 USD Received 7 Jul 2010; revised 13 Aug 2010; accepted 15 Sep 2010; published 4 Oct 2010

by one well defined ring, see Fig. 11. Note that the spatial extension of the pattern was smaller than in all previous positions.

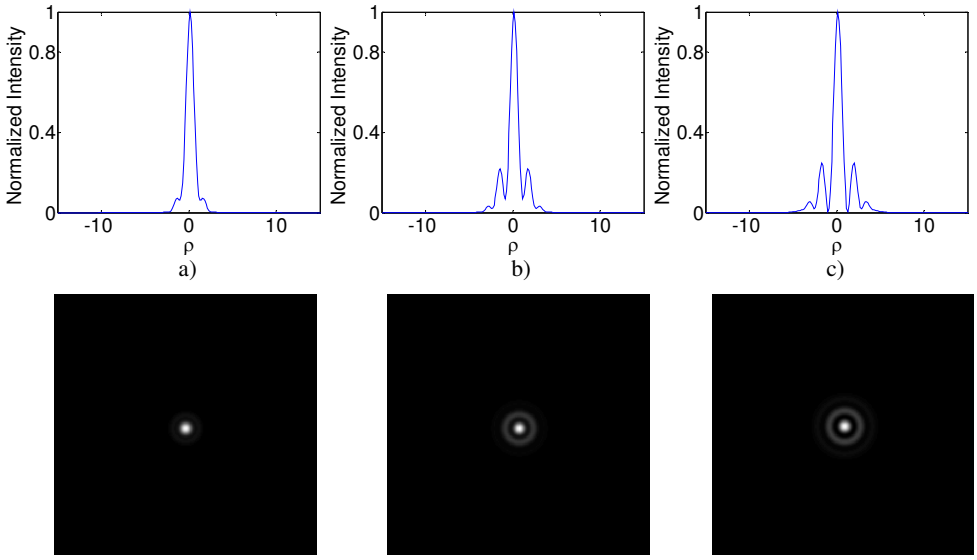

Fig. 11. Far field intensity profiles (upper row) and cross sections (lower row) obtained for a sample with $\Delta\varphi_0 = 2\pi$ rad, set at $z = 2z_0$. And different values of m: a) 1, b) 2 and c) 4.

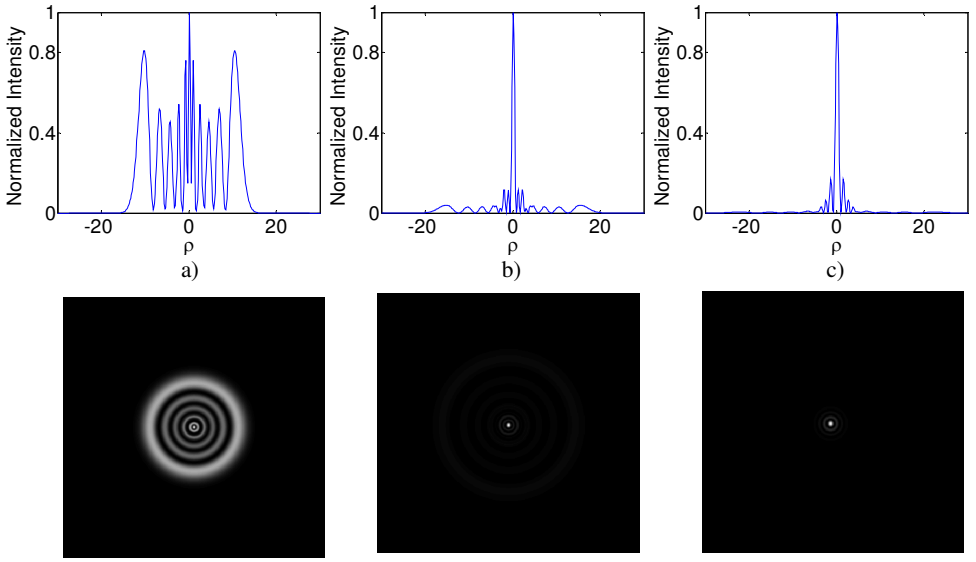

Fig. 12. Far field intensity profiles (upper row) and cross sections (lower row) obtained for a sample with $\Delta\varphi_0 = 12\pi$ rad, set at $z = 2z_0$. And different values of m: a) 1, b) 2 and c) 4.

When the sample was set at $z = 2z_0$ and $\Delta\varphi_0 = 12\pi$ rad, the far field patterns presented a central bright spot and many rings. For $m = 1$ the number of rings was close to that corresponding to the magnitude of the nonlinear phase shift; the outermost and innermost rings were of the highest intensity. When the magnitude of m was increased, two sets of rings were observed, the inmost with higher frequency and intensity than the outer. See Fig. 12.

#130856 - $15.00 USD Received 7 Jul 2010; revised 13 Aug 2010; accepted 15 Sep 2010; published 4 Oct 2010

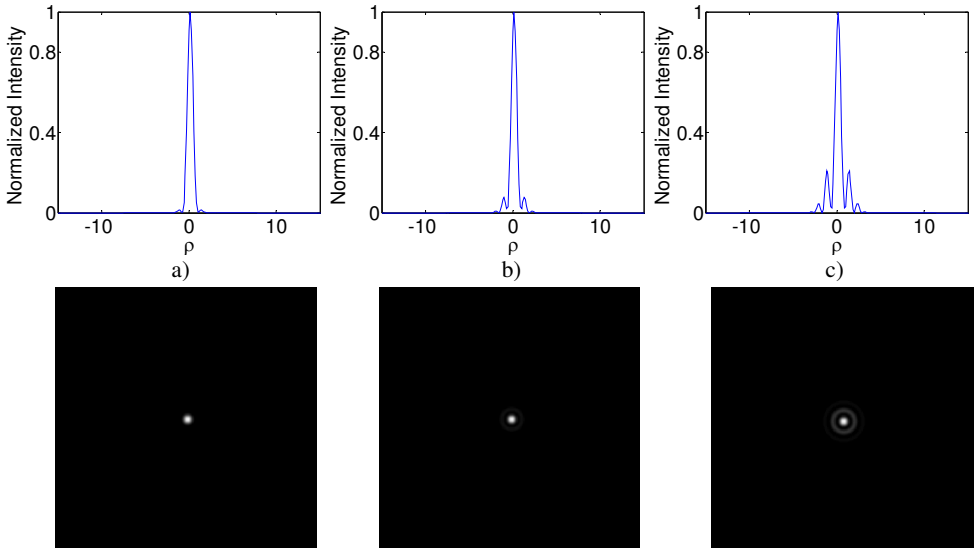

Fig. 13. Far field intensity profiles (upper row) and cross sections (lower row) obtained for a sample with $\Delta\varphi_0 = 2\pi$ rad, set at $z = 4z_0$. And different values of m: a) 1, b) 2 and c) 4.

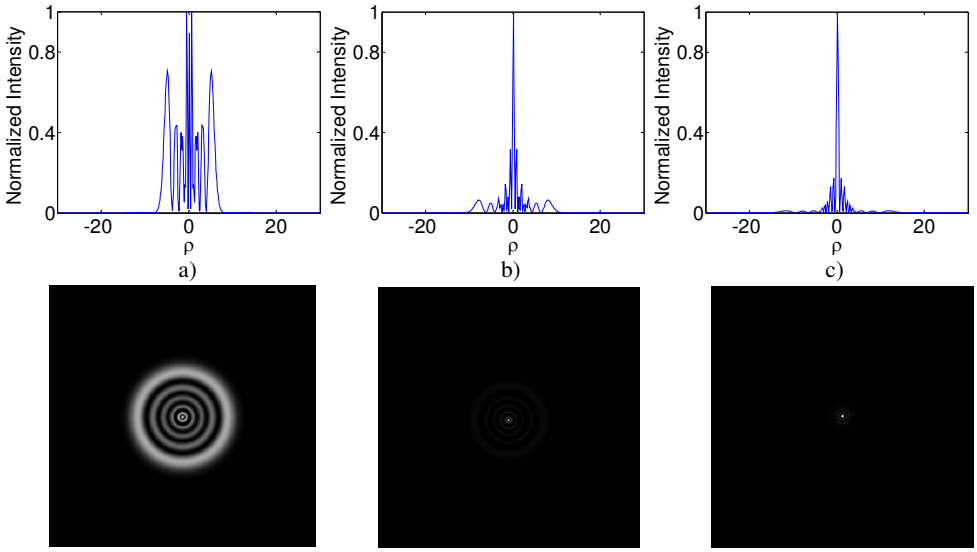

Fig. 14. Far field intensity profiles (upper row) and cross sections (lower row) obtained for a sample with $\Delta\varphi_0 = 12\pi$ rad, set at $z = 4z_0$. And different values of m: a) 1, b) 2 and c) 4.

When the sample was set at $z = 4z_0$ with $\Delta\varphi_0 = 2\pi$ rad, no remarkable differences were observed in the far field patterns with respect to $z = 2z_0$; a central bright spot was obtained for all values of m. A well defined ring surrounding the central spot was obtained for $m = 4$, see Fig. 13. The spatial extensions of the patterns were smaller than in all previous positions.

For the same position and for a sample with $\Delta\varphi_0 = 12\pi$ rad, two set of rings were observed, one with higher frequency and amplitude than the other, see Fig. 14. In all cases a central bright spot was obtained and the number of observed rings does not correspond to the phase shift.

#130856 - $15.00 USD Received 7 Jul 2010; revised 13 Aug 2010; accepted 15 Sep 2010; published 4 Oct 2010

Note that for a negative sign of the nonlinearity the results are the same to the presented here changing the sign of the position. This means that the patterns obtained for a negative nonlinear sample with positive curvature radius of the wavefront are the same to that presented for negative values of z.

It is important to mention that some intensity distributions obtained for some position and *m* values are similar to that obtained for another position and other *m* value. For example, the pattern presented in Fig. 6b is qualitatively similar to that presented in Fig. 10a, for large nonlinear phase shift, or Fig. 3c is qualitatively similar to 5b, for small nonlinear phase shift. However, in order to determine the nonlocality associated to some unknown sample it is necessary to obtain its far field patterns behavior to different positions and curvature radius of the wavefront of a Gaussian beam.

4. Conclusions

We have presented a model where the effects of the nonlocality in the photoinduced phase change is taken into account as a parameter that can take different values depending on the extension of the photoinduced refractive index change. The model considers a Gaussian incident intensity distribution and a thin sample. The far field intensity distributions were calculated numerically for different: 1) positions of the sample respect to the waist of the Gaussian beam, 2) maximum nonlinear phase shifts and 3) different values of the extension of the photoinduced refractive index. The numerical results demonstrate that for positive curvature radius of the wavefronts a central bright spot is always obtained for a positive nonlinear media and a central dark spot is not always obtained for a negative one. For a negative curvature radius of the wavefronts a central bright spot is always obtained for a negative nonlinear media and a central dark spot is not always obtained for a positive one. Another important result is that the number of rings in the pattern is not always related to the maximum phase shift; this number depends on the position of the sample respect to the waist of the beam and the nonlocality of the nonlinearity.

From the analysis we can say that our model reproduce in a well correspondence the results reported in media with thermal nonlinearity with the parameter $m = 1$, see as example references [1,2,5,20] where experiments with absorbing media were made. The case $m = 2$ reproduce similar results to that reported in the reference [10]. The case $m = 4$ reproduce similar results to that reported in references [3,9] where samples of liquid crystals were used. Recently a paper where the far field patterns are used to determine the sign and magnitude of the nonlinear refractive index was published [9], we add to their conclusions that it is also possible to know the locality of the nonlinearity. The model is not restricted to only integer numbers for *m*, in fact in some samples different values of *m* must be needed depending on the used wavelength.

Acknowledgements

This work was partially supported by VIEP, BUAP, grant MEOM-EXC10-G. E.V.G.R., acknowledges receipt of a CONACYT, México, fellowship.

#130856 - $15.00 USD Received 7 Jul 2010; revised 13 Aug 2010; accepted 15 Sep 2010; published 4 Oct 2010